Julia Werner, Benjamin Besser, Christoph Brandes, Stephen Kroll, Kurosch Rezwan

Production of ceramic membranes with different pore sizes for virus retention

Production of ceramic membranes with different pore sizes for virus retention

Julia Werner, Benjamin Besser, Christoph Brandes, Stephen Kroll*, Kurosch Rezwan

Advanced Ceramics, University of Bremen, Am Biologischen Garten 2, 28359 Bremen, Germany

ARTICLE INFO

Article history:
Received 27 May 2014
Received in revised form 2 October 2014
Accepted 12 October 2014
Available online 12 November 2014

Keywords:
Extrusion
Ceramic capillary membrane
Pore size
Porosity
Virus retention

ABSTRACT

Porous ceramic capillary membranes made of yttria-stabilised zirconia (YSZ) are presented, which are conditioned for virus filtration by varying the initial YSZ particle size. Compared to polymeric membranes, ceramic membranes offer remarkable advantages for filtration processes as they show excellent chemical, thermal and mechanical stability and can easily be cleaned by backflushing. YSZ powders with different particle sizes (30 nm, 40 nm and 90 nm) are individually and mixed processed by extrusion, dried and finally sintered at 1050 °C for 2 h. The sintered YSZ capillaries are characterised by microstructural analysis including Hg-porosimetry, BET analysis and 3-point bending tests. By increasing the initial YSZ particle size, increased average membrane pore sizes ranging from 24 nm to 146 nm are obtained. Mechanically stable membranes are provided showing high open porosities of ~45% and ~36% for capillaries composed of single and mixed YSZ powders, respectively. By increasing the membrane pore size, reduced virus retention capacities in combination with increased water permeate fluxes are achieved. Capillaries made of YSZ-40 nm ensure both, log reduction values (LRV) ≥ 4 for small model bacteriophages MS2 and PhiX174 and high water permeate fluxes (~30 L/(m^2 hbar)), being suitable for sustainable virus filtration as requested by the World Health Organisation (WHO) and the United States Environmental Protection Agency (USEPA). Due to long-term virus filtration for two weeks, membrane pore plugging is successfully avoided by iterative backflushing and relatively high membrane fluxes in combination with requested LRV 4 level fulfilling the virus filter criterion are achieved.

1. Introduction

Water is essential to life, but today, 783 million people still have an inadequate access to clean drinking water [1]. Especially in developing countries, an access to safe drinking water and sanitation is not ensured, e.g. for 46% of the population in Oceania and 39% of the population in Sub-Sahara Africa [1,2]. According to the World Health Organisation (WHO), 1.8 million people die annually from diseases such as diarrhoea, cholera and dysentery transmitted through polluted water [3,4].

The three main contaminations for water pollution are of chemical (e.g. heavy metals, organic and inorganic species), physical (e.g. colour) and biological (e.g. bacteria and viruses) origin [5]. The biological pollutants are the most frequent and deadly contaminations in the drinking water of developing countries, because waterborne diseases are mainly caused by viruses (e.g. adenovirus, enterovirus, rotaviruses, hepatitis A and E virus) and bacteria (e.g. *Vibrio cholerae*, *Escherichia coli*, *Salmonella enterica*) [2,5,6].

Nowadays, water disinfection methods to inactivate viruses are based on physical or chemical processes. Conventional methods to inactivate viruses in water are heat treatment techniques, chemical treatments using free chlorine or chlorine dioxide, and the application of ozone or UV-irradiation. Especially for heat and chemical treatments, a virus inactivation can be achieved, but high costs and the potential production of toxic disinfection by-products (DBPs) are given at the same time. Ozone treatments and UV-irradiations can induce virus inactivation, but high investment costs and trained personal are required [7–11].

A promising alternative for water disinfection is the filtration which is based on removing suspended solids from a fluid by passing it through a permeable fabric (e.g. membranes). Filtration is based on size exclusion effects and therefore, contaminants which are larger than the membrane pore size can be effectively retained [12,13]. A virus removal using ceramic filters made of raw materials (e.g. diatomaceous earth) or chemically synthesised ceramics (e.g. zirconia) is possible as shown by several authors [14–16]. To ensure a high virus removal even for pore sizes larger than the viruses a pretreatment by coagulation/flocculation was performed by other authors [17–20]. Beside size exclusion methods particularly functionalised ceramic particles (e.g. amino-silanised)

* Corresponding author. Tel.: +49 421 218 64933; fax: +49 421 218 64932.
E-mail address: stephen.kroll@uni-bremen.de (S. Kroll).

http://dx.doi.org/10.1016/j.jwpe.2014.10.007

and ceramic components (e.g. MgO-doped, colloidal zirconia) are applied for virus adsorption to enhance the virus titre reduction. [21–23]

Today, polymeric membranes possess high water permeate fluxes combined with required high virus retention levels [24,25]. Compared to polymeric membranes, ceramic membranes show excellent chemical, thermal and mechanical stability. The importance of porous ceramic membranes is increasing in water purification, because monomodal and narrow pore size distributions in the meso- and macroporous range can be tailored depending on applied processing parameters (e.g. initial ceramic particle size, shaping technique, drying and sintering conditions). Because of their high mechanical strength ceramic membranes can withstand high pressure loads and therefore, they are able to endure high water permeate flux rates. Another advantage of ceramic membranes is that they can easily be cleaned by backflushing, thermal, acidic or basic treatment without affecting the pore morphology [26]. In addition, ceramic membranes do not show any swelling behaviour during water filtration maintaining their structural compactness. In contrast to polymeric membranes, the production costs of ceramic membranes are 3 up to 5 times higher, but this can be compensated by their longer lifetime of up to ten years instead of one year for polymeric membranes [27]. Further disadvantages of ceramic membranes are their brittle behaviour and higher material weight compared to polymeric membranes [28].

For a highly efficient virus filtration it is necessary that a reliable pore size of the membrane of less than or equal to virus size is provided to act as a mechanical filter based on size exclusion principle. Viruses are the smallest pathogens and have diameters between 20 and 300 nm [6]. Therefore, virus removal can be attained by ultrafiltration showing pore sizes in the range between 2 and 100 nm, that is, mesoporous and lower macroporous range [29]. To ensure high virus removal capacities, pore sizes less than the virus are preferred leading to low water permeate fluxes [15,30,31]. Based on the guidelines from WHO and United States Environmental Protection Agency (USEPA) a log-reduction value of 4 (i.e. at least 99.99 percent (4-log) removal) is required to fulfil the virus filter criterion providing safe and clean drinking water. The generation of tubular ceramic membranes offering both, a reliable cut-off for virus retention in combination with high open porosities and water permeate fluxes, is challenging and requires in-depth knowledge of the whole processing route.

The aim of this work is to extrude yttria-stabilised zirconia (YSZ) capillaries for virus filtration that feature ideally pore sizes and porosities for realising high virus retention capacities of LRV $\geq$4 in combination with high water permeate fluxes. YSZ was chosen because of its high fracture toughness and strength compared to other ceramic oxide materials (e.g. alumina). The effect of initial YSZ powders showing different particle sizes on the membrane microstructure (pore size, open porosity, specific surface area), mechanical stability (bending strength) and water permeate flux were analysed in detail. Virus retention capacities of the extruded and finally sintered capillary membranes were determined by virus filtration tests in dead-end mode using two small bacteriophages, MS2 and PhiX174, which served as surrogates for human pathogenic viruses. Finally, long-term virus filtration tests for two weeks were performed applying iterative backflushing to control the membrane fouling.

2. Materials and methods

2.1. Materials

The yttria-stabilised zirconia (YSZ) powders and reagents were purchased from commercial sources and used as received. Three different YSZ powders were used: VP Zirkonoxid 3-YSZ (YSZ-30 nm, Lot. 3157061469, specific surface area = 40 ± 15 m^2/g, particle size < 30 nm) was purchased from Evonik Industries, Germany, TZ-3Y-E (YSZ-40 nm, Lot. Z302131P, specific surface area = 16 ± 3 m^2/g, particle size = 40 nm) and TZ-3YS-E (YSZ-90 nm, Lot. S300886P, specific surface area = 7 ± 2 m^2/g, particle size = 90 nm) were obtained from Krahn Chemie GmbH, Germany.

3-Aminopropyltriethoxysilane (APTES, 99%, product number 440140, Lot. SHBC8357V), magnesium chloride hexahydrate ($MgCl_2$, product number M2670, Lot. BCBJ3659V), polyvinyl alcohol (PVA, fully hydrolysed, product number P1763, Lot. SLBC9027V), sodium chloride (NaCl, product number S7653, Lot. SZBC2560V), tryptic soy agar (TSA, product number 22091, Lot. BCBG4777V) and culture media tryptic soy broth (TSB, product number T8907, Lot. 109K0165) were obtained from Sigma–Aldrich Chemie GmbH, Germany.

For virus retention tests we used the bacteriophage MS2 (DSM Cat. No. 13767) and its host bacteria *E. coli* (DSM Cat. No. 5210) as well as the bacteriophage PhiX174 (DSM Cat. No. 4497) and its host bacteria *E. coli* (DSM Cat. No. 13127) from German Collection of Microorganisms and Cell Cultures (DSMZ), Germany.

All experiments were carried out using double-deionised water with an electrical resistance of 18 MΩ, which was obtained from a Synergy® apparatus (Millipore, Germany).

2.2. Characterisation of YSZ powders

The particle properties of three different YSZ powders, namely VP Zirkonoxid 3-YSZ (YSZ-30 nm), TZ-3Y-E (YSZ-40 nm) and TZ-3YS-E (YSZ-90 nm), were characterised determining the particle size distribution, density, specific surface area and zeta-potential. Particle size distributions and average particle sizes (d_{50}-values) were determined by acoustic spectroscopy (DT 1200, Dispersion Technology) using ceramic suspensions containing 1 vol.% particles. An ultrasonic treatment was applied for 10 min at 240 W with a pulse rate of 0.5 s (ultrasonic finger, Branson Sonifier 450, Heinemann, Germany) to deagglomerate the YSZ powders before the measurement. The acoustic spectroscopy was taken out at pH 3 to ensure a particle rejection, because YSZ has an isoelectric point (IEP) in the neutral to low basic pH range ($IEP_{YSZ} = \sim 7–9$) [32].

Additionally, transmission electron microscopy (TEM, FEI Titan 80/300) was performed to estimate the particle size and morphology. The density of the three different YSZ powders was analysed by helium pycnometry (Pyconmatic ATC, Porotec). The specific surface area was obtained by nitrogen adsorption according to BET method (BELSORP-Mini, BEL Japan Inc.) after degassing the YSZ powders using argon for at least 3 h at 120 °C followed by flushing with dry argon. Zeta-potential measurements (DT 1200, Dispersion Technology) with suspensions containing 1 vol.% particles were performed to determine the IEPs of the YSZ powders. The pH titration was carried out with an integrated titration unit using 1 M HCl or 1 M KOH.

2.3. Fabrication of YSZ capillaries by extrusion

Fig. 1 shows the processing route for the fabrication of YSZ capillaries by extrusion. The fabrication is divided into four main parts involving slurry preparation, shaping by extrusion process, drying of the extruded capillaries and finally, sintering of the obtained green capillaries.

2.3.1. Slurry preparation

As shown in Fig. 1, four components were used to prepare the ceramic slurry: YSZ powder as ceramic material, APTES as dispersant, PVA as binder and double-deionised water as solvent. As already described by Qui et al., PVA was used because of the low

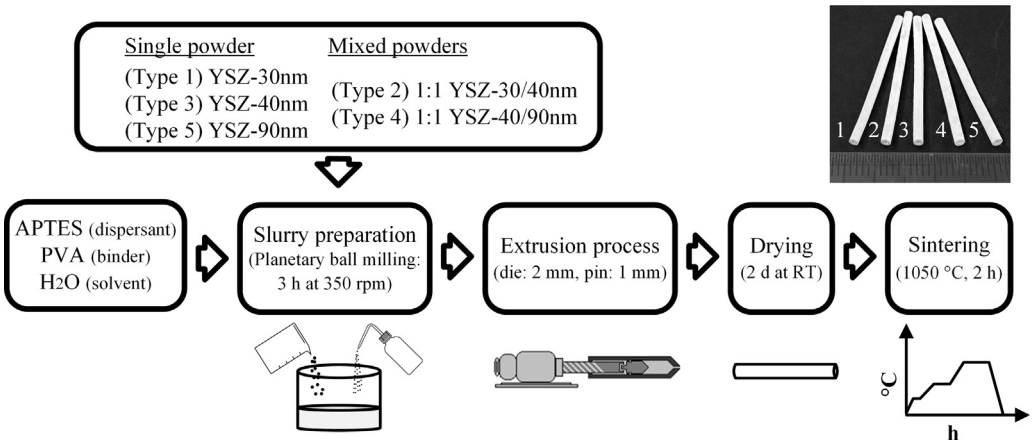

Fig. 1. Processing route for the fabrication of porous YSZ capillaries sintered at 1050 °C for virus filtration based on initial YSZ powders with different particle sizes.

risk of crack-formation during the drying of extruded capillaries made of YSZ [33]. Based on the manufacturer data, the primary particle size of the used YSZ powders ranged from 30 nm to 90 nm. Five different types of capillaries were prepared. Three capillary types were all based on one YSZ powder, namely Type 1 (made of YSZ-30 nm), Type 3 (made of YSZ-40 nm) and Type 5 (made of YSZ-90 nm), respectively. The two other capillary types were composed of two of the three YSZ powders. The powders were mixed in a ratio of 1:1 (w/w) and the capillaries were named Type 2 (based on YSZ-30 nm and YSZ-40 nm powder) and Type 4 (based on YSZ-40 nm and YSZ-90 nm powder), respectively. To create extrudable slurries showing different initial particle sizes, individual slurry compositions for each YSZ particle type were used. For one batch (i.e. one grinding vessel of the planetary ball mill), the amount of YSZ powder as well as the amount of the binder (PVA) was kept constant at 132 g and 8 g, respectively. To provide stabilised and homogeneous YSZ slurries for the extrusion process following slurry compositions were used: For the preparation of Type 1 capillaries, 44.4 g water and 7.4 g APTES for the preparation of Type 2 capillaries, 38 g water and 5.7 g APTES and for the preparation of Type 3, Type 4 and Type 5 capillaries 33 g water and 4 g APTES were used. The solid contents of the prepared feedstocks were then 72.9 wt.% (Type 1), 76.2 wt.% (Type 2) and, 79.1 wt.% (Types 3–5), respectively.

The preparation of the slurry in the planetary ball mill (PM400, Retsch) was performed in the same way for each YSZ powder. Each of two grinding vessels was filled with the reagents (YSZ powder, PVA, APTES and water) and 50 alumina grinding balls with a diameter of 10 mm. The slurry was milled for 3 h at 350 rpm changing the rotation direction every 5 min. Afterwards, the grinding balls were removed from the slurry and the slurry was transferred to the extruder.

2.3.2. Extrusion process

The extrusion was carried out with a self-made laboratory extruder as described in our previous works [15,34]. The extruder consisted of a spindle drive with shaft joint which was connected to a press ram, a convenient vessel for the slurry uptake, an extrusion die with integrated pin and a conveyor band for depositing the extruded capillaries. The extruder was equipped with an extrusion die of 2.0 mm diameter and an integrated pin with 1.0 mm diameter.

2.3.3. Drying and sintering

The extruded capillaries were dried for at least two days at RT to remove residual solvents. Afterwards, these green capillaries were sintered for 2 h at 1050 °C with preceding dwell times at 280 °C and 500 °C to remove the dispersant (APTES) and binder (PVA) molecules, respectively (Nabertherm, Germany). According to our previous studies based on YSZ, a moderate sintering temperature of 1050 °C for 2 h was chosen to obtain capillary membranes showing both, relatively high open porosities in combination with a sufficient mechanical stability [15,35]. After sintering, the capillaries were ready for characterisation.

2.4. Characterisation of extruded green and sintered YSZ capillaries

2.4.1. Structural and mechanical membrane properties

The sintering shrinkage was determined by measuring the outer and inner diameter of the sintered (1050 °C for 2 h) capillary membranes by optical microscopy (VHX-600DSO, Keyence). For each capillary type ten samples were tested for statistical significance. The pore size distribution, the average pore size (d_{50}) and the open porosity of the sintered samples were analysed by Hg-porosimetry (Mercury Porosimeter Pascal 140 and 440, POROTEC GmbH). In addition to the experimental determination of the pore size, the d_{50} pore size (d_{pore50}) assuming a random dense packing (1) and a random loose packing (2) of processed ceramic particles was calculated based on the simulation of Gotoh et al. [36] where a_{50} is the particle size:

$$d_{pore50} = 0.46 \cdot a_{50} \quad (1)$$

$$d_{pore50} = 0.48 \cdot a_{50} \quad (2)$$

The specific surface area of the sintered capillaries was determined by nitrogen adsorption according to BET method after degassing the capillaries for at least 3 h at 120 °C using argon. Furthermore, the sintered capillaries were analysed by scanning electron microscopy (SEM, Field-emission SEM SUPRA 40, Zeiss) to visualise the microstructure of the outer capillary surface and to check the presence of potential macro- and microdefects.

The mechanical strength of the sintered capillaries was measured by 3-point bending tests according to DIN EN 843-1 (Roell Z005, Zwick). The testing machine was equipped with a load cell for 5 kN. The applied velocity was 0.4 mm/min. A capillary with a length of 12 mm was placed in the centre of the sample holder and tested. The distance between the sample holder and the support rollers (L) was 8 mm. To calculate the bending strength σ_F, the following equation was used:

$$\sigma_F = \frac{8 \cdot F \cdot L \cdot OD}{\pi \cdot (OD^4 - ID^4)} \quad (3)$$

In this equation, F is the measured force at which fracture takes place; OD is the outer and ID the inner diameter of the capillary. For

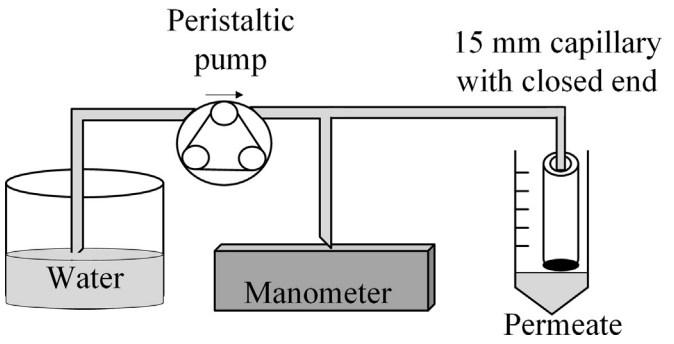

Fig. 2. Experimental set-up of the water permeate flux test.

each sintered capillary type 30 samples were tested for statistical significance. The statistical analysis was based on the maximum-likelihood method.

2.4.2. Water permeate flux

The water permeate flux of the sintered YSZ capillaries was determined by intracapillary water feeding operating in dead-end mode where double-deionised water served as feed solution. Intracapillary water feeding was achieved by a peristaltic pump (BVP Standard, Ismatec) applying different pressures in the range between 25 and 500 mbar to force the water through the membrane. Therefore, one end of the capillary was sealed with silicon (Wirosil Dublier-Silikon, BEGO Medical GmbH) and the other end was connected with a convenient silicon tubing to the peristaltic pump (Fig. 2). Based on adjustable flow rates mediated by the peristaltic pump a manometer was used to determine the applied pressures (C9500, COMARK). For each membrane type (Types 1–5), three individual capillaries with a length of 1.5 cm were tested operating in vertical orientation. The active filtering area of the sintered capillaries is 0.40 cm^2. The applied filtration time for membrane samples fabricated with YSZ-40 nm and YSZ-90 nm was 30 min for each applied pressure (Type 3, Type 4 and Type 5). Due to low water permeate fluxes of capillary membranes derived from capillaries based on YSZ-30 nm powder (Type 1 and Type 2) filtration times up to one day were applied. The permeated water volumes were obtained by weight measurement (ABJ, Kern & Sohn GmbH). Each measurement was performed in triplicate.

The error due to water evaporation during gravimetric measurements at RT was 0.8 ± 0.2% for membranes made of YSZ-40 nm as well as YSZ-90 nm (30 min filtration time) and 14.7 ± 4.6% for membranes consisting of YSZ-30 nm (24 h filtration time).

2.4.3. Virus retention test

The virus retention of the sintered capillaries was tested using two small bacteriophages which served as surrogates for human pathogenic viruses: MS2 and PhiX174. MS2 is a single-stranded RNA virus with a diameter of 25–27 nm and an IEP of 3.9 [12,37]. PhiX174 is a single-stranded DNA virus with a diameter of 26–32 nm and an IEP of 6.6 [12,37]. These viruses belong to the smallest viruses and therefore, filtrations based on size exclusion principle can be ideally investigated.

The virus retention test was performed as described in our previous study [15] with slight modifications. In short, the preparation of the virus feed solutions was done by virus propagation for MS2 and PhiX174, respectively, and the bacteriophages were separately propagated in their specific host bacteria (*E. coli*). Virus containing saline solutions (0.02 M $MgCl_2$/0.15 M NaCl) at pH 5.8 served as viral feed solution showing initial virus concentrations of around 10^9 PFU/mL.

The virus retention test was performed in dead-end mode and virus containing solutions were intracapillary fed to single capillary membranes with an accessible length of 1.5 cm. For each filtration test, new single sintered capillary membranes were used (Types 1–5) and intracapillary virus feeding was performed at an applied pressure of 500 mbar until a permeate volume of 15 mL was reached. For each membrane type, three individual capillary membranes were tested in parallel (triplicate determination).

The bacteriophages in the feed solution and permeate were enumerated using the plaque-forming-unit (PFU) method according to the procedure as described in our previous work [15]. The PFU method was performed using 5 mL feed and permeate solution, respectively, and virus quantification was done in triplicate. The dosage of bacteriophage stocks was aimed to reach a final concentration of 10^9 PFU/mL and therefore, theoretically detectable virus retention was LRV of 9 which is equivalent to a percental value of 99.9999999%.

2.4.4. Long-term virus filtration

Long-term virus filtration tests for a period of two weeks were performed using the experimental set-up as shown in Fig. 2 with the exception that a virus containing solution instead of water served as feed. The long-term filtration test was performed in dead-end mode and a MS2 containing solution with a concentration of 10^9 PFU/mL was intracapillary fed at an applied pressure of 500 mbar to a single capillary membrane (Type 3) with a length of 1.5 cm. For statistical significance four individual capillary membranes were used in parallel (fourfold determination). Every day (i.e. after a filtration time of 24 h) the water permeate flux and the transmembrane pressure were determined and the virus retention capacity of each capillary was analysed by plaque test. Backflushing was applied after the membrane flux reached a threshold level less than 5 L/(m^2 hbar). Therefore, a pulsating backflush was performed for a period of 3 h using a $MgCl_2$ (pH 5.8) solution. The capillary was therefore alternating backflushed at an applied pressure of 1000 mbar for 20 min and flushed forward at an applied pressure of 500 mbar for 2 min. The capillary was finally backflushed for 21 h at an applied pressure of 1000 mbar being ready for a new filtration cycle. The virus feed solution was replaced after each backflushing cycle by a new prepared MS2 solution showing a concentration of 10^9 PFU/mL. The long-term virus filtration experiment was performed for two weeks and three backflushing cycles for membrane cleaning were applied (after day 4, 8 and 12, respectively).

3. Results and discussion

3.1. Properties of YSZ powders

TEM was performed to analyse the size, surface and morphology of used YSZ particles and the results are shown in Fig. 3 presenting TEM images of YSZ-30 nm (A1), YSZ-40 nm (B1) and YSZ-90 nm (C1). According to the manufacturer data, the specified primary particle sizes of <30 nm, 40 nm and 90 nm can be confirmed by TEM analyses. All YSZ particles have a spherical shape and the tendency to form agglomerates.

In addition to TEM measurements, particle size distributions and average particle sizes (d_{50}-values) of the YSZ powders were quantified by acoustic spectroscopy. These quantitative results are shown in Fig. 3 for the different powders in form of YSZ-30 nm (A2), YSZ-40 nm (B2) and YSZ-90 nm (C2). All powders have a bimodal particle size distribution where the first peak at lower particle sizes <1 μm represents the primary particle size and possible small agglomerations, respectively. The second peak at particle sizes >1 μm indicates larger agglomerations composed of several YSZ particles. In agreement with the manufacturer data, increased particle sizes in the following order were obtained: YSZ-30 nm < YSZ-40 nm < YSZ-90 nm. The determined average particle

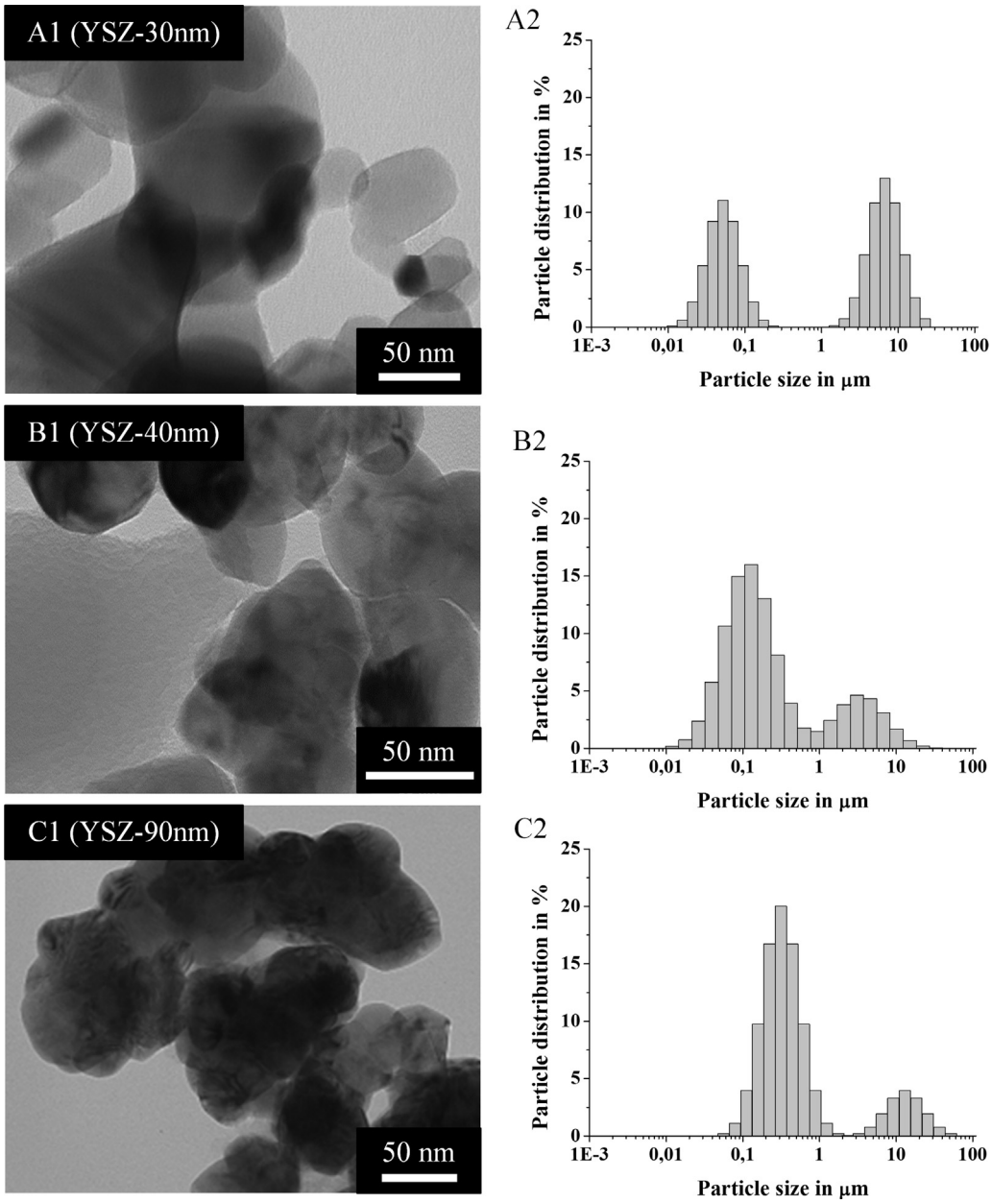

Fig. 3. TEM images (1) and particle size distributions (2) obtained by acoustic spectroscopy for (A) YSZ-30 nm powder, (B) YSZ-40 nm powder and (C) YSZ-90 nm powder.

sizes (d_{50}) in relation to first peaks were 55 nm, 122 nm and 310 nm, respectively. Compared to specified primary YSZ particle sizes of the manufacturers, increased d_{50}-values (first peaks) by factor 1.7–3.4 were obtained assuming particle aggregation which can be confirmed by TEM analyses (Fig. 3 A1–C1).

The second peak of the bimodal particle size distributions is attributed to greater agglomerates >1 μm. Fig. 3 shows, that the tendency to form agglomerates decreases with increasing YSZ particle sizes. Hence, the intensity of the second peaks decreases in the following order: YSZ-30 nm > YSZ-40 nm > YSZ-90 nm. However, under consideration of agglomeration, the YSZ particle sizes specified by the manufacturers can be confirmed by qualitative TEM analyses and quantitative acoustic spectroscopy measurements.

Table 1 summarises the results of the acoustic spectroscopy measurements for the powders YSZ-30 nm (VP Zirkonoxid 3-YSZ, Evonik Industries), YSZ-40 nm (TZ-3Y-E, Krahn Chemie GmbH) and YSZ-90 nm (TZ-3YS-E, Krahn Chemie GmbH) in comparison to the manufacturer data. In addition, the density, specific surface area and IEPs of YSZ powders are given.

The density of the powders YSZ-30 nm, YSZ-40 nm and YSZ-90 nm which was measured by helium pycnometry is 5.7 g/cm^3 and 5.8 g/cm^3, respectively, and these values are in agreement with the density of 3 mol% (~5 wt.%) YSZ powders indicated by the manufacturer. As expected, YSZ powders with increasing particle sizes show decreased specific surface areas and determined values of 39.4 ± 0.8 m^2/g (YSZ-30 nm), 14.4 ± 0.2 m^2/g (YSZ-40 nm) and 6.6 ± 0.1 m^2/g (YSZ-90 nm) are in accordance with the information specified by the manufacturers. Based on zeta potential measurements the IEPs of YSZ-30 nm, YSZ-40 nm and YSZ-90 nm are 7.3, 9.0 and 8.2, respectively, and thus, IEPs of YSZ powders at neutral or rather slight basic pH values are obtained which is as expected for YSZ particles doped with 3 mol% yttria.

Table 1
Properties of used YSZ powders (YSZ-30 nm, YSZ-40 nm and YSZ-90 nm powder).

	Product name Company Abbreviation of YSZ powder types	VP Zirkonoxid 3-YSZ Evonik Industries YSZ-30 nm	TZ-3Y-E Tosoh Corporation[a] YSZ-40 nm	TZ-3YS-E Tosoh Corporation[a] YSZ-90 nm
Manufacturer's data	Primary particle size (nm)	<30	40	90
	Density (g/cm^3)	n/a	6.1	6.1
	Specific surface area (m^2/g)	40 ± 15	16 ± 3	7 ± 2
	IEP (−)	7.1	8.6	8.5
Measurements	Particle size (nm) (bimodal distribution): peak 1; peak 2	55; 6700	122; 3080	310; 13000
	Density (g/cm^3)	5.7	5.8	5.8
	Specific surface area (m^2/g)	39.4 ± 0.8	14.4 ± 0.2	6.6 ± 0.1
	IEP (−)	7.3	9.0	8.2

[a] YSZ powders were produced from Tosoh Cooperation, Inc. (Japan) and sold by Krahn Chemie GmbH (Germany).

3.2. Properties of extruded YSZ capillaries

3.2.1. Sintering shrinkage

The outer diameter (OD) and inner diameter (ID) of the sintered (1050 °C for 2 h) capillaries were measured by optical microscopy. The initial size of the capillaries after the extrusion was equal to the dimensions of used extrusion die (2.0 mm diameter) and integrated pin (1.0 mm diameter).

Fig. S1 (Supplementary information) compares the measured outer and inner diameters of the capillaries in the sintered state made of different YSZ powders varying in their particle size. The sintering shrinkage implies the shrinkage after drying and sintering and therefore, it is equal to the total shrinkage. As expected, all capillary types shrink during drying as well as during sintering. The highest shrinkage is detected for the Type 1 and Type 2 capillaries which were based on the lowest YSZ particle size (YSZ-30 nm or rather a mixture of YSZ-30 nm and YSZ-40 nm), because relatively high specific surface areas of around 39.4 m^2/g and 14.4 m^2/g (Table 1) are responsible for the induction of increased particle-particle-contacts and for the driving force during sintering. The outer as well as the inner diameter were reduced to around 80% of their initial size due to applied sintering at 1050 °C for 2 h. The outer diameter of both capillary types is 1.65 ± 0.04 mm and the inner diameter changed to 0.80 ± 0.04 mm. In contrast to the capillaries made of YSZ-40 nm and YSZ-90 nm (Types 3–5), no difference between the shrinkage of the outer and inner diameter was determined.

Compared to capillaries made of YSZ-30 nm (Type 1), samples based on only YSZ-40 nm (Type 3) or only YSZ-90 nm (Type 5) show significantly reduced shrinkage values. These two capillary membranes show a similar shrinkage behaviour. After sintering at 1050 °C for 2 h, the capillaries made of YSZ-40 nm (Type 3) and YSZ-90 nm (Type 5) have an outer diameter of approximately 92–95% and an inner diameter of approximately 84–89 % compared to their initial geometrical dimensions. The Type 4 capillaries which are based on both, YSZ-40 nm and YSZ-90 nm powder, show a higher shrinkage in comparison to the capillaries based on only one of these powders, but a lower shrinkage compared to the capillaries based on YSZ-30 nm powder (Type 1 and Type 2). The shrinkage after sintering is 86% for the outer diameter and around 80% for the inner diameter.

3.2.2. Pore size distribution and open porosity

Ceramic capillary membranes were fabricated using initial YSZ powders differing in their particle size (YSZ-30 nm, YSZ-40 nm and YSZ-90 nm) and both individual and mixed YSZ powders were used for membrane fabrication resulting in sintered capillaries with high contour accuracy (Fig. 1). In addition to the macroscopic overview, Fig. 4 presents the microstructures of the outer capillary surface obtained by SEM (A1-E1). Here, the pores are uniformly distributed within the YSZ matrix and as expected, increased pore sizes are achieved by the processing of YSZ powders with increased particle sizes (Type 1 < Type 2 < Type 3 < Type 4 < Type 5). Quantification of the pore size distribution, average pore diameter (d_{50}) and open porosity for all capillary types 1–5 was achieved by Hg-porosimetry as shown in parts A2-E2 of Fig. 4. The sintered capillary membranes based on both single YSZ powders (Type 1, 3 and 5) and mixed YSZ powders (Type 2 and 4) show monomodal pore size distributions.

According to SEM analyses, increasing the initial YSZ particle size led to increased pore sizes of the capillary membrane. In relation to used YSZ powders in form of YSZ-30 nm (Type 1), 1:1 YSZ-30/40 nm (Type 2), YSZ-40 nm (Type 3), 1:1 YSZ-40/90 nm (Type 4) and YSZ-90 nm (Type 5) pore size distributions are obtained from 10 to 40 nm (A2), 10 to 60 nm (B2), 20 to 100 nm (C2), 20 to 500 nm (D2) and 50 to 500 nm (E2). The determined average pore diameters were 24 nm, 35 nm, 57 nm, 96 nm and 146 nm, respectively, which can be attributed to the mesoporous and lower macroporous range.

Parts A2-E2 of Fig. 4 show that the open porosity of the capillary membranes made of single and mixed YSZ powders is in a similar range of around 47–55%. Thereby, a relatively high content of the open porosity up to 11% can be attributed to pore sizes >0.1 μm (A2, B2, C2) and >0.5 μm (D2, E2), respectively. The intruded Hg volume representing this porosity content can be related to surface inhomogeneities of the capillary membrane and the inner channel of the capillary (lumen). Thus, the open porosity which exclusively represents the pore sizes of the capillary membranes composed of individual YSZ powders (Type 1, 3 and 5, respectively) is approximately 42–45%. Here, the initial particle size has no significant influence on the membrane open porosity because of the random arrangement of uniform YSZ particles during processing (YSZ-30 nm, YSZ-40 nm and YSZ-90 nm, respectively). In contrast, the capillary membranes composed of mixed YSZ powders (Types 2 and 4) show lower open porosities of around 36% considering relevant pore sizes <0.5 μm. This reduction of the open porosity can be attributed to a higher particle packing density where smaller particles can fill the 'gaps' (i.e. pores) between bigger particles. The tendency to form high particle densities is further strengthened by capillary membranes made of YSZ-30 nm and YSZ-90 nm where pore sizes are mesoporous and low open porosities of ~30% are evident, being not suitable for the application of high performance membranes for virus filtrations (data not shown).

Table 2 summarises the results achieved by Hg-porosimetry compared to calculated average membrane pore sizes which show a good matching with the measured ones. Additionally, the specific surface areas obtained by BET analyses and bending strengths obtained by 3-point bending tests are presented. In agreement with determined pore sizes, the specific surface area of the capillary

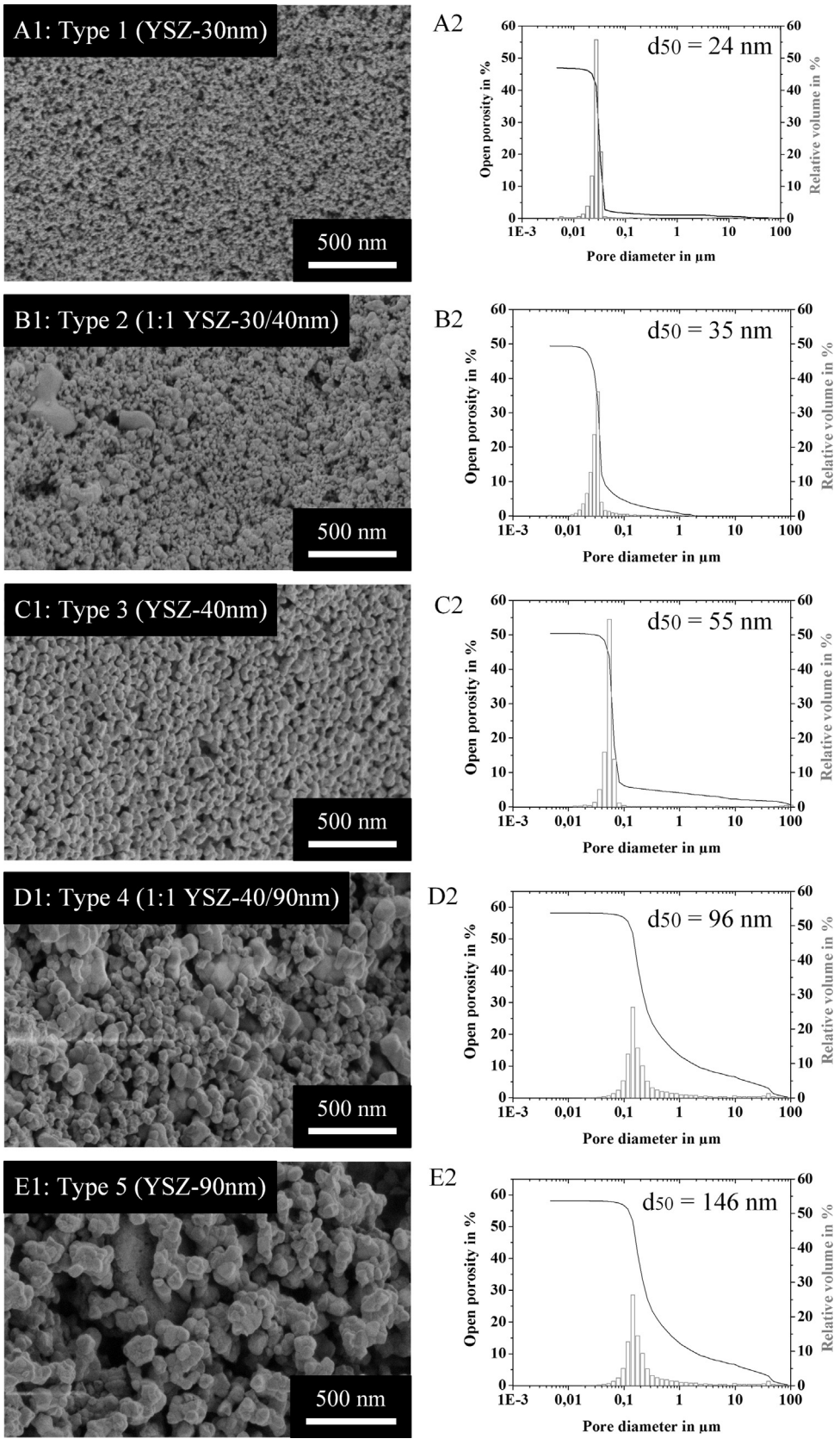

Fig. 4. Microstructures of the outer capillary surface (1) and pore size distributions as well as open porosities (2) of YSZ capillaries sintered at 1050 °C for 2 h based on different initial YSZ powders. (A) YSZ-30 nm capillary, (B) capillary made of YSZ-30 nm and YSZ-40 nm, (C) YSZ-40 nm capillary, (D) capillary made of YSZ-40 nm and YSZ-90 nm and (E) YSZ-90 nm capillary.

Table 2
Membrane properties of YSZ capillaries sintered at 1050 °C based on different initial YSZ powders.

Parameter	YSZ capillary type				
	Type 1 (YSZ-30 nm)	Type 2 (1:1 YSZ-30/40 nm)	Type 3 (YSZ-40 nm)	Type 4 (1:1 YSZ-40/90 nm)	Type 5 (YSZ-90 nm)
Hg-porosimetry					
Pore diameter (nm)	10–40	10–50	20–100	20–300	50–500
Measured d_{50} (nm)	24.0 ± 2.6	35.0 ± 1.0	55.3 ± 3.2	96.0 ± 2.6	146.0 ± 4.4
Calculated d_{50} based on random close packing (nm)[a]	25.3	n.d.	56.1	n.d.	142.6
Calculated d_{50} based on random loose packing (nm)[b]	26.4	n.d.	58.6	n.d.	148.8
Open porosity (%)[c]	42.8 ± 2.6	35.6 ± 1.7	42.1 ± 3.0	34.1 ± 2.6	45.4 ± 2.7
BET method					
Specific surface area (m^2/g)	21.9 ± 2.6	16.3 ± 0.1	10.0 ± 0.4	8.4 ± 0.1	5.5 ± 0.0
3-point bending test					
Bending strength (MPa)	38.0	28.1	26.3	12.9	9.2
Weibull modulus m (−)	6.2	6.6	8.2	6.1	5.2

[a] Average pore diameters for capillaries made of single YSZ powders are calculated according to Eq. (1) based on the work from Gotoh et al. [36].
[b] Average pore diameters for capillaries made of single YSZ powders are calculated according to Eq. (2) based on the work from Gotoh et al. [36].
[c] Based on the intruded Hg volume the determined open porosity is related to the pore size range representing exclusively the pores in the membrane (<0.5 μm).

membranes significantly decreased with increasing pore sizes from values of 21.87 ± 2.57 m^2/g (Type 1) to 5.51 ± 0.01 m^2/g (Type 5). Here, an increase of the average pore size from 24 nm to 146 nm (factor ~6) results in a decrease of the specific surface area of the capillaries by a factor of ~4. As expected, the bending strength of the YSZ capillary membranes strongly decreased with increasing membrane pore sizes. Bending strength values for σ_0 from 38.0 MPa (Type 1) to 9.2 MPa (Type 5) were determined. A moderate sintering temperature of 1050 °C for 2 h was chosen to achieve ceramic capillary membranes showing both, high open porosities >~35% which are necessary for high performance filtration applications and sufficient mechanical stabilities to endure high pressure loads during filtration. To obtain the highest possible strength level for porous ceramic oxide membranes yttria-stabilised zirconia (YSZ) was used even if it is more expensive compared to alumina. As written by Park [38] the strength of ceramics depends on the porosity as shown in the following equation (Ryshkewitch's equation [39]):

$$\sigma = \sigma_0 e^{-np} \quad (4)$$

where σ is the strength of a porous material, σ_0 is the pore free strength, p is the volume fraction of porosity and n is an integer ($n = 4 \sim 7$).

As specified by the manufacturers the used YSZ powders have a bending strength of 1200 MPa for dense sintered bodies. The bending strength for dense sintered alumina is around 500 MPa [38]. Considering the Ryshkewitch's equation this higher bending strength by a factor of 2.4 for nonporous YSZ will have an influence on the strength of the porous body. The Weibull modulus m is in a range between 8.2 and 5.2 which is a value quite normal for porous structures compared to other authors who worked with porous ceramic materials [40–42]. Based on capillary membranes showing the highest average pore size of 146 nm in combination with an open porosity of approximately 45%, the bending strength reached nearly 10 MPa, being already suitable for sample handling and filtration applications.

3.2.3. Water permeate flux

Fig. 5 presents the water permeate fluxes of all YSZ capillary membrane types (Types 1–5) as a function of applied pressure. As expected, water permeate fluxes are increased with increasing applied pressures for all YSZ capillary membranes. In agreement with determined pore sizes and open porosities of the capillaries (Fig. 4 and Table 2), water permeate fluxes are increased in the following order: Type 5 (~450 L/(m^2 hbar)) > Type 4 (~110 L/(m^2 hbar)) > Type 3 (~30 L/(m^2 hbar)) > Type 2 (~5 L/(m^2 hbar)) > Type 1 (~3 L/(m^2 hbar)). Compared to the capillary membrane made of YSZ-30 nm (Type 1) considerable higher water permeate fluxes by a factor of around 150 are achieved for the capillaries made of YSZ-90 nm (Type 5). To realise both high water permeate fluxes and a performance reliability during virus filtration operating in dead-end mode an adequate pressure of 500 mbar was applied for all membrane types.

3.2.4. Virus retention

Two small bacteriophages, namely MS2 (25–27 nm) and PhiX174 (26–32 nm), were used to quantify the virus retention capacity of the YSZ capillaries sintered at 1050 °C for 2 h. The virus filtration was performed in dead-end mode by intracapillary virus feeding.

Fig. 6 shows the results of the virus retention performance. As expected, each type of the YSZ capillary membranes (Type 1–5) shows a similar retention behaviour for MS2 and PhiX174, because these viruses have nearly the same size. The capillary made of YSZ-30 nm (Type 1) shows a LRV of 9.2 ± 0.4 for MS2 and 8.5 ± 0.9 for PhiX174 fulfilling the virus filter criterion (LRV ≥ 4). Based on the mesoporous membrane structure featuring an average pore diameter of 24 nm and an open porosity of 45% (Fig. 4 A2) the viruses can

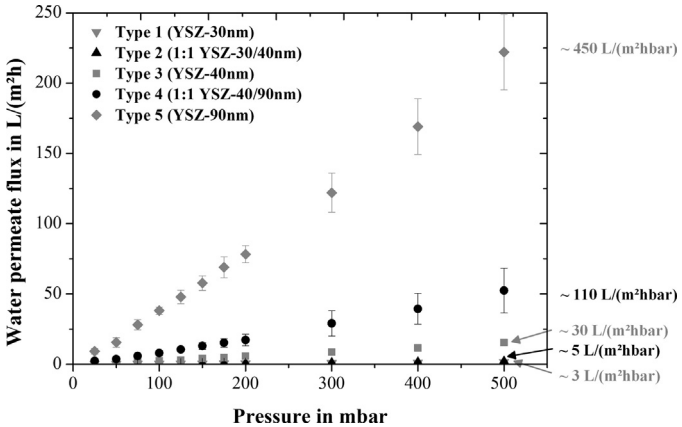

Fig. 5. Determination of water permeate flux at different applied pressures using YSZ capillaries sintered at 1050 °C based on different initial YSZ powders.

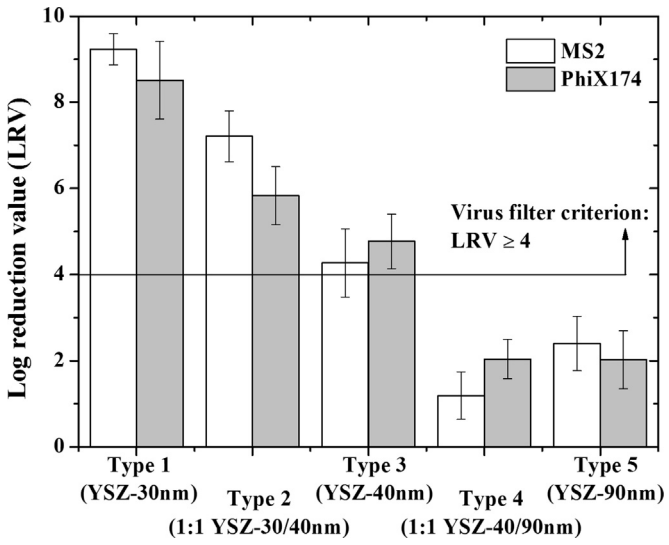

Fig. 6. Retention of two small bacteriophages in form of MS2 and PhiX174 mediated by YSZ capillaries sintered at 1050 °C based on different initial YSZ powders. Virus feed concentrations were 10^9 PFU/mL.

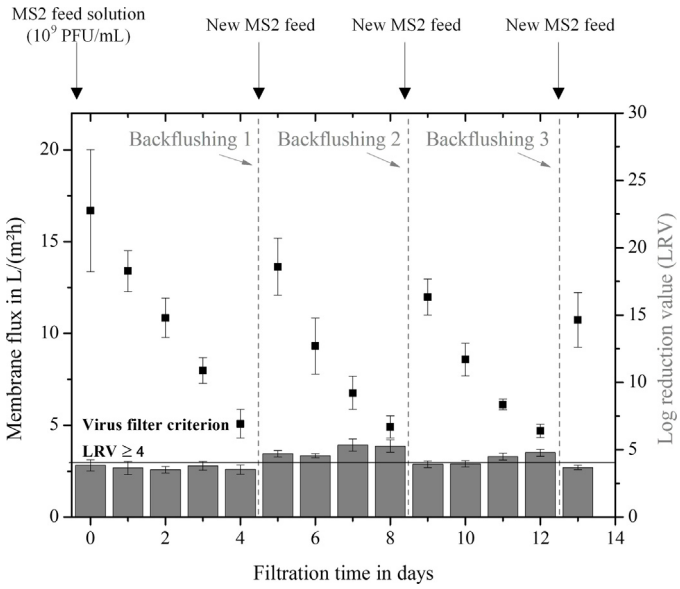

Fig. 7. Long-term virus filtration with capillary membranes made of YSZ-40 nm (Type 3) determining both the water permeate flux and the virus retention capacity as a function of the filtration time. MS2 was used as model virus showing feed concentrations of 10^9 PFU/mL and applied transmembrane pressures were 500 mbar.

be efficiently retained by size exclusion. By increasing the membrane pore size reduced virus retention capacities are obtained resulting in LRVs of around 6–7 (Type 2), 4.5 (Type 3) and 2 (Types 4 and 5, respectively). The processing of powder mixtures of YSZ-40 nm and YSZ-90 nm (Type 4) as well as the single YSZ-90 nm powder (Type 5) results in macroporous membranes with average pore diameters of 96 nm and 146 nm (Fig. 4D2 and E2), respectively, which are nearly four and six times higher than the virus diameters. Therefore, these capillary membranes cannot fulfil the virus filter criterion of LRV ≥ 4, being not suitable for virus filtration applications. However, based on used capillaries made of YSZ-40 nm (Type 3) both the required LRV of at least 4 is fulfilled for MS2 (4.3 ± 0.8) and PhiX174 (4.8 ± 0.6) and relatively high water permeate fluxes of ~30 L/(m^2 hbar) (Fig. 5) are achieved providing a promising candidate for long-term virus filtration. Compared to the Type 5 capillaries (450 L/(m^2 hbar)) the Type 3 capillaries show reduced water permeate flux values by a factor of 15, but the virus retention capacity of the membrane is fulfilled (LRV ≥ 4). The Type 5 capillaries made of YSZ-90 nm are promising membrane candidates due to their high flux properties if the membrane surface characteristics are adequately adjusted for virus adsorption (e.g. wet-chemical aminosilanisation, membrane doping with metal oxides (MgO)).

Today, polymer membranes (e.g. PVDF) as presented in the study by El Hadidy et al. [24] show both a high virus retention capacity combined with a high water permeate flux. However, compared to ceramic membranes polymeric membranes show no high chemical, thermal and mechanical stability. Therefore, ceramic membranes can easily be cleaned by backflushing (where high pressure loads are applied), thermal, acidic or basic treatment without affecting the pore morphology [26]. Consequently, cleaned ceramic capillary membranes maintain their integrity and they can be used for a high number of filtration cycles without losing their membrane performance. In contrast to polymeric membranes, the production costs of ceramic membranes are 3 up to 5 times higher, but this can be compensated by their longer lifetime of up to ten years instead of one year for polymeric membranes [27].

3.2.5. *Long-term virus filtration test*

Fig. 7 shows the results of the long-term virus filtration test for two weeks using Type 3 capillaries (YSZ-40 nm) and the bacteriophage MS2 to analyse the pore blocking behaviour during filtration (membrane fouling) and the membrane regeneration potential mediated by backflushing. In agreement with determined water permeate fluxes at an applied pressure of 500 mbar for capillary membranes made of YSZ-40 nm (Fig. 5 and Type 3) an initial membrane flux of 16.7 L/(m^2 h) (day 0) is obtained. By virus filtration for four days the membrane flux is stepwise reduced to 5 L/(m^2 h) (factor ~3) whereas LRVs of around 4 were evident during filtration (after day 1, day 2, day 3 and day 4, respectively) ensuring a reliable virus retention by size exclusion. Backflushing was applied after four filtration days resulting in a membrane flux value of 13.6 L/(m^2 h) which is marginally lower compared to the initial membrane flux (day 0). However, retained viruses at the membrane surface which were responsible for pore plugging can be successfully removed by backflushing and cleaned capillary membranes are provided for a new virus filtration cycle. Due to the second and third filtration cycle from day 4–8 and day 8–12, respectively, the membrane fluxes are decreased with increasing filtration times and the membrane virus retention capacities are slightly increased of around 11% and 19%, respectively, based on membrane fouling and the associated pore plugging by retained viruses. The fouled capillary membranes can be regenerated by applied backflushing steps. Membrane fluxes of 12.0 L/(m^2 h) and 10.7 L/(m^2 h) are obtained after second and third backflushing procedure, respectively, while the virus retention capacities of the capillary membranes are not really affected by both increased filtration times and backflushing showing LRVs of around 4. Compared to the initial membrane flux (day 0) a flux reduction of 36% is obtained after the third backflushing step (day 13) still fulfilling the virus filter criterion after a filtration time of nearly two weeks which is required by WHO and USEPA to guarantee save drinking water.

4. Conclusion

This study demonstrates the possibility to fabricate YSZ capillary membranes with adjustable pore size by extrusion for controlled virus retention. The effect of the initial YSZ particle size on the capillary properties was analysed in detail focussing on the macro- and microstructure. Based on the achieved results the YSZ-phase and the pores were uniformly distributed forming two interpenetrating networks with the individuals (particles and pores). Increasing

the initial YSZ particle size led to an increased pore size of the capillary membrane. By utilisation of different YSZ powders (single versus mixed powders) showing primary particle sizes of 30 nm, 40 nm and 90 nm, average pore sizes of the capillary membranes of 24 nm (Type 1 made of YSZ-30 nm), 35 nm (Type 2 made of YSZ mixture of YSZ-30 nm/40 nm), 55 nm (Type 3 made of YSZ-40 nm), 96 nm (Type 4 made of YSZ mixture of YSZ-40/90 nm) and 146 nm (Type 5 made of YSZ-90 nm) were generated. A sintering at moderate temperatures of 1050 °C for 2 h induced the formation of sintering necks between single YSZ particles generating capillary microstructures with relatively high open porosities of ~45 % for capillary membranes made of single YSZ powders and ~36 % for capillary membranes made of mixed YSZ powders in combination with a sufficient mechanical stability for filtration applications.

Based on adjustable membrane pore sizes in the meso- and lower macroporous range, the virus filtration efficiency can be controlled where increased pore sizes led to higher permeate fluxes, but at the same time to reduced virus retention capacities. Fulfilling the virus filter criterion of at least 4 LRV level in combination with high flow capacities, capillaries made of YSZ-40 nm (Type 3) are promising candidates for sustainable virus filter systems. Here, small bacteriophages in form of MS2 and PhiX174 were efficiently retained (LRV of 4.3 and 4.8, respectively) and water permeate fluxes of around 30 L/(m^2 hbar) were obtained. Under consideration of the initial particle size of the used ceramic powder, the presented processing route represents a versatile tool for the fabrication of tubular ceramic membranes with reliable cut-offs for virus filtration applications.

However, the capillaries made of a mixture of YSZ-40/90 nm and YSZ-90 nm (Type 4 and Type 5), respectively, which do not fulfil the virus filter criterion can be advantageously used for high flux filtration applications if an adequate adsorption capacity for viruses by a membrane surface functionalisation is provided. Beside conventional chemical membrane functionalisation strategies (e.g. silanisations) the direct integration of metal oxides (e.g. FeO, MgO) during slurry preparation can open up new perspectives on analysing the interactions between viruses and modified ceramic surfaces under flow conditions. A long-term virus filtration test for two weeks using Type 3 capillaries (YSZ-40 nm) showed that a membrane regeneration can be successfully applied by backflushing maintaining relatively high membrane fluxes in combination with requested LRV 4 level by WHO and USEPA fulfilling the virus filter criterion.

Acknowledgements

This work was supported by German Research Foundation (DFG, Reference number KR 3902/2-2, Project title "Nanostructured ceramic membranes with tailored functionalisation and geometry for virus filtration"). We thank Petra Witte (University of Bremen, Department of Geosciences) for her support with the SEM.

Appendix A. Supplementary data

Supplementary data associated with this article can be found, in the online version, at doi:10.1016/j.jwpe.2014.10.007.

References

[1] United Nations, The Millennium Development Goals Report 2012, United Nations, New York, 2012.
[2] J.P.S. Cabral, Water microbiology: bacterial pathogens and water international, J. Environ. Res. Public Health 7 (2010) 3657–3703.
[3] World Health Organization, The World Health Report 2005, Make every mother and child count, WHO Press, Geneva, 2005.
[4] K. Onda, J. LoBuglio, J. Bartram, Global access to safe water: accounting for water quality and the resulting impact on MDG progress, Int. J. Environ. Res. Public Health 9 (2012) 880–894.
[5] A. Gadgil, Drinking water in developing countries, Annu. Rev. Energy Environ. 23 (1998) 253–286.
[6] R.D. Arnone, J.P. Walling, Waterborne pathogens in urban watersheds, J. Water Health 5 (1) (2007) 149–162.
[7] T. Clasen, L. Haller, D. Walker, J. Bartram, S. Cairncross, Cost-effectiveness of water quality interventions for preventing diarrhoeal disease in developing countries, J. Water Health (2007) 599–608.
[8] M.A. Shannon, P.W. Bohn, M. Elimelech, J.G. Georgiadis, B.J. Marinas, A.M. Mayes, Science and technology for water purification in the coming decades, Nature 452 (2008) 301–310.
[9] H. Junli, W. Li, R. Nenqi, L.X. Li, S.R. Fun, Y. Guanle, Disinfection effect of chlorine dioxide on viruses, algae and animal planktons in water, Water Res. 31 (1997) 455–460.
[10] World Health Organization, Managing Water in the Home: Accelerated Health Gains from Improved Water Supply, WHO, Geneva, 2002.
[11] G. Ko, T.L. Cromeans, M.D. Sobsey, UV inactivation of adenovirus type 41 measured by cell culture mRNA RT-PCR, Water Res. 39 (2005) 3643–3649.
[12] A. Duek, E. Arkhangelsky, R. Krush, A. Brenner, V. Gitis, New and conventional pore size tests in virus-removing membranes, Water Res. 46 (2012) 2505–2514.
[13] I. Voigt, Nanofiltration with ceramic membranes, Chem. Ing. Tech. 77 (2005) 559–564.
[14] B. Michen, F. Meder, A. Rust, J. Fritsch, C. Aneziris, T. Graule, Virus removal in ceramic depth filters based on diatomaceous earth, Environ. Sci. Technol. 46 (2011) 1170–1177.
[15] S. Kroll, M.O.C. de Moura, F. Meder, G. Grathwohl, K. Rezwan, High virus retention mediated by zirconia microtubes with tailored porosity, J. Eur. Ceram. Soc. 32 (2012) 4111–4120.
[16] N. Muhammad, R. Sinha, E.R. Krishnan, C.L. Patterson, Ceramic filter for small system drinking water treatment: evaluation of membrane pore size and importance of integrity monitoring, J. Environ. Eng. 135 (2009) 1181–1191.
[17] T. Meyn, T.O. Leiknes, A. König, MS2 removal from high NOM content surface water by coagulation – ceramic microfiltration, for potable water production, AIChE J. 58 (2012) 2270–2281.
[18] B. Zhu, D.A. Clifford, S. Chellam, Virus removal by iron coagulation–microfiltration, Water Res. 39 (2005) 5153–5161.
[19] L. Fiksdal, T. Leiknes, The effect of coagulation with MF/UF membrane filtration for the removal of virus in drinking water, J. Membr. Sci. 279 (2006) 364–371.
[20] N. Shirasaki, T. Matsushita, Y. Matsui, M. Kobuke, K. Ohno, Comparison of removal performance of two surrogates for pathogenic waterborne viruses, bacteriophage Qβ and MS2, in a coagulation–ceramic microfiltration system, J. Membr. Sci. 326 (2009) 564–571.
[21] F. Meder, J. Wehling, A. Fink, B. Piel, K. Li, K. Frank, et al., The role of surface functionalization of colloidal alumina particles on their controlled interactions with viruses, Biomaterials 34 (17) (2013) 4203–4213.
[22] B. Michen, J. Fritsch, C. Aneziris, T. Graule, Improved virus removal in ceramic depth filters modified with MgO, Environ. Sci. Technol. 47 (2013) 1526–1533.
[23] M. Wegmann, B. Michen, T. Luxbacher, J. Fritsch, T. Graule, Modification of ceramic microfilters with colloidal zirconia to promote the adsorption of viruses from water, Water Res. 42 (2008) 1726–1734.
[24] A.M. ElHadidy, S. Peldszus, M.I. Van Dyke, An evaluation of virus removal mechanisms by ultrafiltration membranes using MS2 and (X174 bacteriophage, Sep. Purif. Technol. 120 (2013) 215–223.
[25] J. Langlet, L. Ogorzaly, J-C. Schrotter, C. Machinal, F. Gaboriaud, J.F.L. Duval, et al., Efficiency of MS2 phage and Qβ phage removal by membrane filtration in water treatment: applicability of real-time RT-PCR method, J. Membr. Sci. 326 (2009) 111–116.
[26] J. Finley, Ceramic membranes: a robust filtration alternative, Filtr. Sep. 42 (2005) 34–37.
[27] E.P. Garmash, Y.N. Kryuchkov, V.N. Pavlikov, Ceramic membranes for ultra- and microfiltration (Review), Glass Ceram. 52 (1995) 150–152.
[28] C.B. Carter, M.G. Norton, Ceramic Materials, Science and Engineering, 1st ed., Springer, New York, 2007.
[29] S.S. Madaeni, A.G. Fane, G.S. Grohmann, Virus removal from water and wastewater using membranes, J. Membr. Sci. 102 (1995) 65–75.
[30] S.S. Madaeni, The application of membrane technology for water disinfection, Water Res. 33 (1999) 301–308.
[31] R. Aronino, C. Dlugy, E. Arkhangelsky, S. Shandalov, G. Oron, A. Brenner, et al., Removal of viruses from surface water and secondary effluents by sand filtration, Water Res. 43 (2009) 87–96.
[32] A.R. Hanifi, M. Zazulak, T.H. Etsell, P. Sarkar, Effects of calcination and milling on surface properties, rheological behaviour and microstructure of 8 mol% yttria-stabilised zirconia (8 YSZ), Powder Technol. 231 (2012) 35–43.
[33] M. Qiu, Y. Fan, N. Xu, Preparation of supported zirconia ultrafiltration membranes with the aid of polymeric additives, J. Membr. Sci. 348 (2010) 252–259.
[34] S. Kroll, L. Treccani, K. Rezwan, G. Grathwohl, Development and characterisation of functionalised ceramic microtubes for bacteria filtration, J. Membr. Sci. 365 (2010) 447–455.
[35] S. Kroll, C. Brandes, J. Wehling, L. Treccani, G. Grathwohl, K. Rezwan, Highly efficient enzyme-functionalized porous zirconia microtubes for bacteria filtration, Environ. Sci. Technol. 46 (2012) 8739–8747.

[36] K. Gotoh, M. Nakagawa, M. Furuuchi, A. Yoshigi, Pore size distributions in random assemblies of equal spheres, J. Chem. Phys. 85 (1986) 3078–3080.
[37] B. Michen, T. Graule, Isoelectric points of viruses, J. Appl. Microbiol. 109 (2010) 388–397.
[38] J. Park, Bioceramics: Properties, Characterization, and Applications, Springer Science and Business Media, LLC, New York, USA, 2008.
[39] E. Ryshkewitch, Compression strength of porous sintered alumina and zirconia, J. Am. Ceram. Soc. 36 (1953) 65–68.
[40] T. Isobe, Y. Kameshima, A. Nakajima, K. Okada, Y. Hotta, Gas permeability and mechanical properties of porous alumina ceramics with unidirectionally aligned pores, J. Eur. Ceram. Soc. 27 (2007) 53–59.
[41] A. Atkinson, A. Selçuk, Mechanical behaviour of ceramic oxygen ion-conducting membranes, Solid State Ionics 134 (2000) 59–66.
[42] C. Brandes, L. Treccani, S. Kroll, K. Rezwan, Gel casting of free-shapeable ceramic membranes with adjustable pore size for ultra- and microfiltration, J. Am. Ceram. Soc. 97 (2014) 1393–1401.